Finite Element Formulation of Periodic Conditions and Numerical Observation of Three-Dimensional Behavior in a Flow

AUTHOR(S):

FUJIMA, Shoichi; FUKASAWA, Yasuji; TABATA, Masahisa

数理解析研究所講究録
第836巻 1993年 113-119

Finite Element Formulation of Periodic Conditions and Numerical Observation of Three-Dimensional Behavior in a Flow

藤間 昌一・深澤 寧司・田端 正久
電気通信大学

Shoichi FUJIMA, Yasuji FUKASAWA and Masahisa TABATA
The University of Electro-Communications

1 Introduction

We have developed a finite element scheme for incompresible Navier-Stokes equations by using an upwind approximation of third order accuracy to the convection term in order to compute high-Reynolds-number flows stably and accurately [1]. We have shown the effectiveness of the scheme by some numerical experiments. In the two-dimensional computation of flows past a circular cylinder, we obtained numerical results showing the decrease and the recovery of the drag coefficients C_D at a high-Reynolds-number region. These behaviors agreed well with experimental results qualitavely, but the obtained values of C_D at high Reynolds numbers were greater than experimental results [2]. At high Reynolds numbers three-dimensional movements appear and it is reported in [3] that the C_Ds obtained by two-dimensional analysis are greater than those by three-dimensional analysis. Our final purpose is to confirm the result by our finite element scheme. In this paper, imposing periodic boundary conditions in the axial direction, we formulate the finite element scheme and observe the three-dimensional behavior of flows.

2 Governing Equations and Boundary Conditions

2.1 Flow Problem around a Circular Cylinder

Let $\hat{\omega}$ be a domain in R^2:

$$\hat{\omega} \equiv \{x; |x| > 1/2\},$$

$\hat{\Omega}$ be a domain in R^3:

$$\hat{\Omega} \equiv \hat{\omega} \times R$$

and T be a positive constant. We consider the incompressible Navier-Stokes equations:

$$\partial u/\partial t + (u \cdot \mathrm{grad})u + \mathrm{grad}\ p = (1/Re)\nabla^2 u, \tag{1}$$

$$\text{div } u \;=\; 0 \tag{2}$$

in $(x,t) \in \hat{\Omega} \times (0,T)$, subject to the rigid wall boundary condition on the cylinder surface:

$$u = (0,0,0) \quad \text{on } \Gamma_0 \equiv \{x; x_1^2 + x_2^2 = (1/2)^2\}, \tag{3}$$

an uniform flow condition at infinity in the x_1, x_2 directions:

$$u = (1,0,0) \quad \text{as } x_1^2 + x_2^2 \to \infty \tag{4}$$

and an initial condition:

$$u = u^0 \quad \text{in } \Omega, \quad \text{at } t = 0, \tag{5}$$

where $u = (u_1, u_2, u_3)$ is the velocity, p is the pressure, Re is the Reynolds number and u^0 is a given velocity.

2.2 Approximate Problem in a Bounded Domain

We consider an approximate problem in a bounded domain to solve by the finite element method.

Let $L_{in}, L_{out}, W > 1/2$ and $H > 0$ be constants, ω be a subdomain of $\hat{\omega}$:

$$\omega \equiv [(-L_{in}, L_{out}) \times (-W, W)] \cap \hat{\omega}$$

and Ω be a subdomain of $\hat{\Omega}$:

$$\Omega \equiv \omega \times (0, H).$$

We consider the equations(1),(2) in $\Omega \times (0,T)$.

We replace the condition(4) by an uniform flow condition on the inflow plane:

$$u = (1,0,0) \quad \text{on } \Gamma_1 \equiv \{x \in \partial\Omega; x_1 = -L_{in}\}, \tag{6}$$

the symmetric conditions on the side planes:

$$u_2 = 0, \quad \tau_1 = \tau_3 = 0 \quad \text{on } \Gamma_2 \equiv \{x \in \partial\Omega; x_2 = \pm W\} \tag{7}$$

and the free stress condition on the outflow plane:

$$\tau = (0,0,0) \quad \text{on } \Gamma_3 \equiv \{x \in \partial\Omega; x_1 = L_{out}\}, \tag{8}$$

where $\tau_i = \sum_{j=1}^{3} \sigma_{ij} n_j$, $i = 1,2,3$, is the stress vector, σ_{ij} is the stress tensor and $n = (n_1, n_2, n_3)$ is the unit outward normal to the boundary.

We assume that the phenomenon has periodicity of period H in the x_3-direction:

$$u(\cdot,\cdot,x_3 + H\ ;\ \cdot) = u(\cdot,\cdot,x_3\ ;\ \cdot), \quad p(\cdot,\cdot,x_3 + H\ ;\ \cdot) = p(\cdot,\cdot,x_3\ ;\ \cdot). \tag{9}$$

Hence we impose periodic boundary conditions for the velocity and the pressure on a bottom plane: $\Gamma_b \equiv \{x \in \partial\Omega; x_3 = 0\}$ and on a top plane: $\Gamma_t \equiv \{x \in \partial\Omega; x_3 = H\}$.

3 Programming of Periodic Boundary Conditions

The assembled finite element equations are

$$(\overline{M}/\tau)u_h^{n+1} + B^T p_h^n = r^n, \tag{10}$$
$$Bu_h^{n+1} = 0, \tag{11}$$

in the matrix form, where $\overline{M}$ is the lumped mass matrix, B is the 'divergence' matrix, τ is the time step, u_h^n, p_h^n are the values of u_h, p_h at time $n\tau$ and r^n is a known vector.

We rewrite these equations for introducing periodic boundary conditions,

$$\begin{bmatrix} A_{TT} & A_{TI} & A_{TB} \\ A_{IT} & A_{II} & A_{IB} \\ A_{BT} & A_{BI} & A_{BB} \end{bmatrix} \begin{bmatrix} x_T \\ x_I \\ x_B \end{bmatrix} = \begin{bmatrix} b_T \\ b_I \\ b_B \end{bmatrix}, \tag{12}$$

where x_T, x_I and x_B are unknown values at the points on the top plane, in the interior of the domain and on the bottom plane, respectively. The first(resp. last) row corresponds to the natural boundary condition on the top(resp. bottom) plane.

Now we impose the periodic conditions to eq.(12). We add the first row of eq.(12) to the last row,

$$\begin{bmatrix} A_{TT} & A_{TI} & A_{TB} \\ A_{IT} & A_{II} & A_{IB} \\ A_{BT}+A_{TT} & A_{BI}+A_{TI} & A_{BB}+A_{TB} \end{bmatrix} \begin{bmatrix} x_T \\ x_I \\ x_B \end{bmatrix} = \begin{bmatrix} b_T \\ b_I \\ b_B+b_T \end{bmatrix}, \tag{13}$$

and replace the first row by the periodic boundary conditions,

$$\begin{bmatrix} I & 0 & -I \\ A_{IT} & A_{II} & A_{IB} \\ A_{BT}+A_{TT} & A_{BI}+A_{TI} & A_{BB}+A_{TB} \end{bmatrix} \begin{bmatrix} x_T \\ x_I \\ x_B \end{bmatrix} = \begin{bmatrix} 0 \\ b_I \\ b_B+b_T \end{bmatrix}. \tag{14}$$

Sweeping out the first column, we get

$$\begin{bmatrix} A_{II} & A_{IB}+A_{IT} \\ A_{BI}+A_{TI} & A_{BB}+A_{TB}+A_{BT}+A_{TT} \end{bmatrix} \begin{bmatrix} x_I \\ x_B \end{bmatrix} = \begin{bmatrix} b_I \\ b_B+b_T \end{bmatrix}, \tag{15}$$

which leads a symmetric system of linear equations in x_I and x_B.

The other essential boundary conditions in (3),(6),(7) are imposed to Eq.(15) afterwards.

4 Numerical Results

We used a domain Ω such that $L_{in} = 2.25$, $L_{out} = 6.75$, $W = 2.165$ and $H = 1$. Combining a triangular subdivision of the domain ω(the total number of elements is 678) and the division of $(0, H)$ into m equi-intervals (m =4 or 6), we subdivided the domain Ω to the union of triangular prisms. Finite element subdivision was generated by dividing further each prism into three tetrahedrons. The subdivision in the case of $m = 6$ is shown in Fig.1.

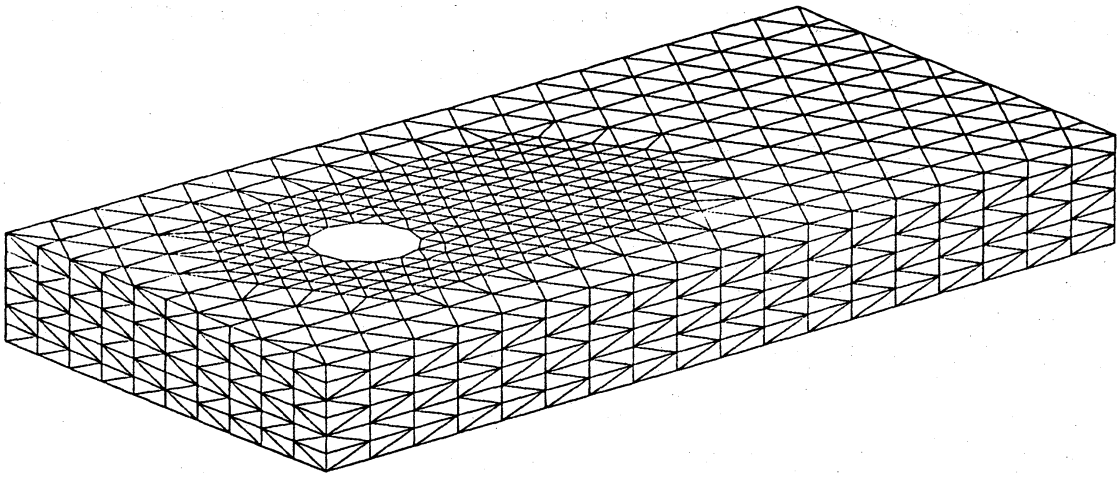

Figure 1: Finite element subdivision, $m = 6$.

The obtained subdivisions are symmetric with respect to the plane: $x_2 = 0$ and the planes: $x_3 = iH/m(i = 0, \cdots, m-1)$, where symmetric solutions with respect to those planes may appear. But they are not uniform in the x_3-direction because of the character of tetrahedral elements.

We used the Karman vortex shedding result of the corresponding two-dimensional computation as the initial datum u^0 for each computation. A small disturbance: $g(t) = \frac{a}{2}(1 - \cos(\pi t))$ was added to the x_3-component of the velocity for $0 \leq t \leq 2$ to see the 'final' state of the solution more quickly. We observed the solution sufficiently afterwards ($t \geq 0$) where the effect of the disturbance was considered to disappear. (We have checked that the results are almost independent of $a(0 \sim 0.5)$ later enough.) We computed the cases $Re = 100$ and $Re = 1000$.

We show the results in the case of $Re = 1000, m = 6$ in Figs.2 ~5. In Fig.2 the velocity vectors on the horizontal planes x_3 =0 and 0.5 are plotted at a moment when the lift coefficient of the cylinder attains a relative maximum. The velocity vectors on the vertical planes $x_2 = 0$ and ± 0.866 are plotted in Fig.3. The pressure contours on the same planes are also plotted in Fig.4 and Fig.5. We can observe that movement in the x_3-direction appears and the flow patterns are different in the horizontal planes.

In the computation of $m = 4$ or the case of $Re = 100$, we could not observe such three-dimensional behavior clearly. In Table.1 we show relative variations of u_1, u_2, p in the x_3-direction:

$$e_i = \max_{\omega}\left(\max_{x_3}|u_i - \overline{u_i}|\right) / \max_{\omega}|\overline{u_i}|, \quad i = 1, 2,$$

$$e_p = \max_{\omega}\left(\max_{x_3}|p - \overline{p}|\right) / \max_{\omega}|\overline{p}|,$$

and the relative quantity of u_3:

$$e_3 = \max_{\Omega}|u_3| / \max_{\Omega}|u|,$$

where $\overline{u_i}$ and $\overline{p}$ are mean values in the x_3-direction at each point in ω. We can see again that three-dimensional behavior is large in the cse of $Re = 1000, m = 6$. In the case of

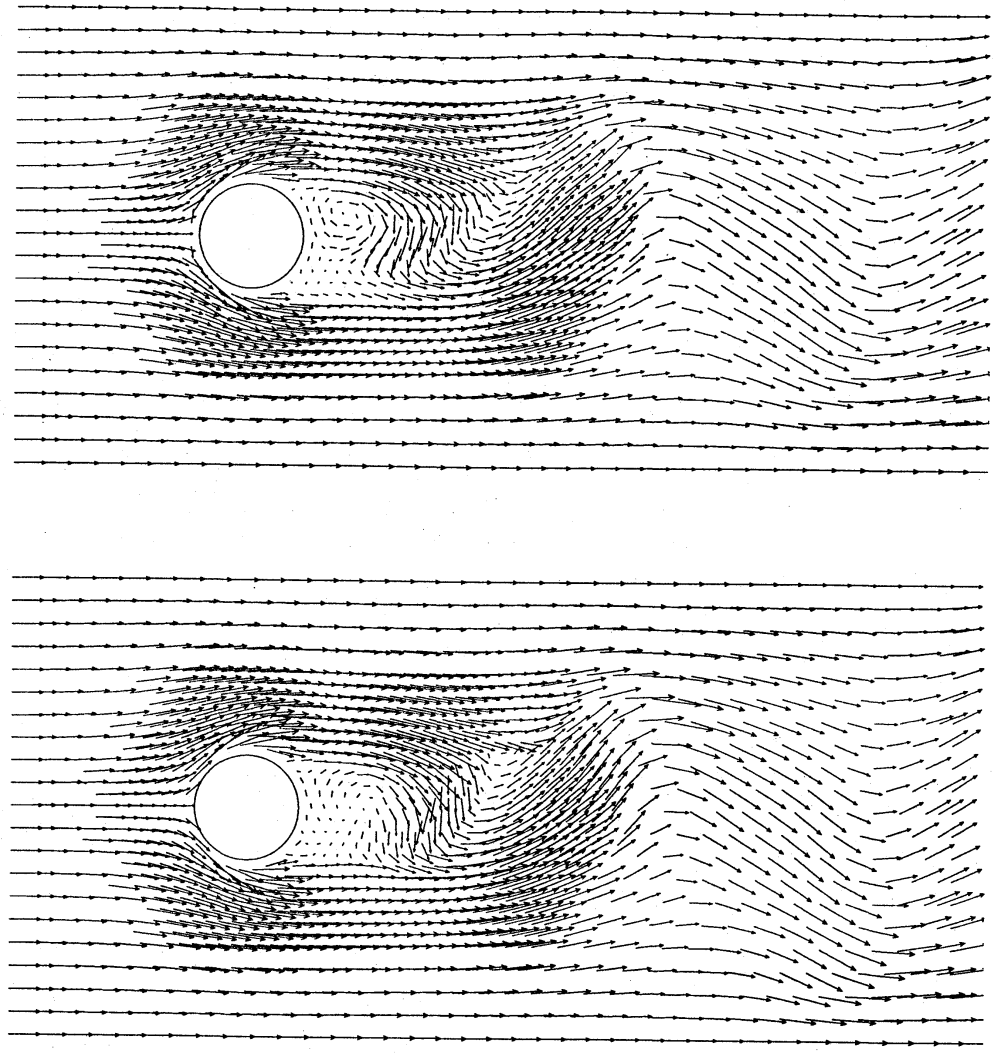

Figure 2: Velocity vectors, $Re = 1000$, $t = 82.28$, $x_3 = 0$(upper) and 0.5(lower).

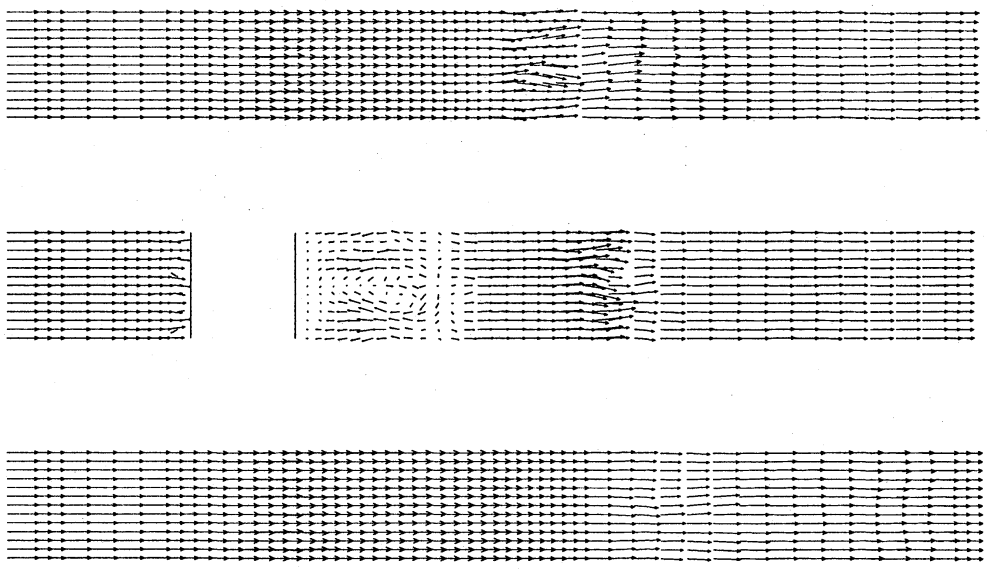

Figure 3: Velocity vectors, $Re = 1000$, $t = 82.28$, x_2 =0.866, 0 and -0.866(from top).

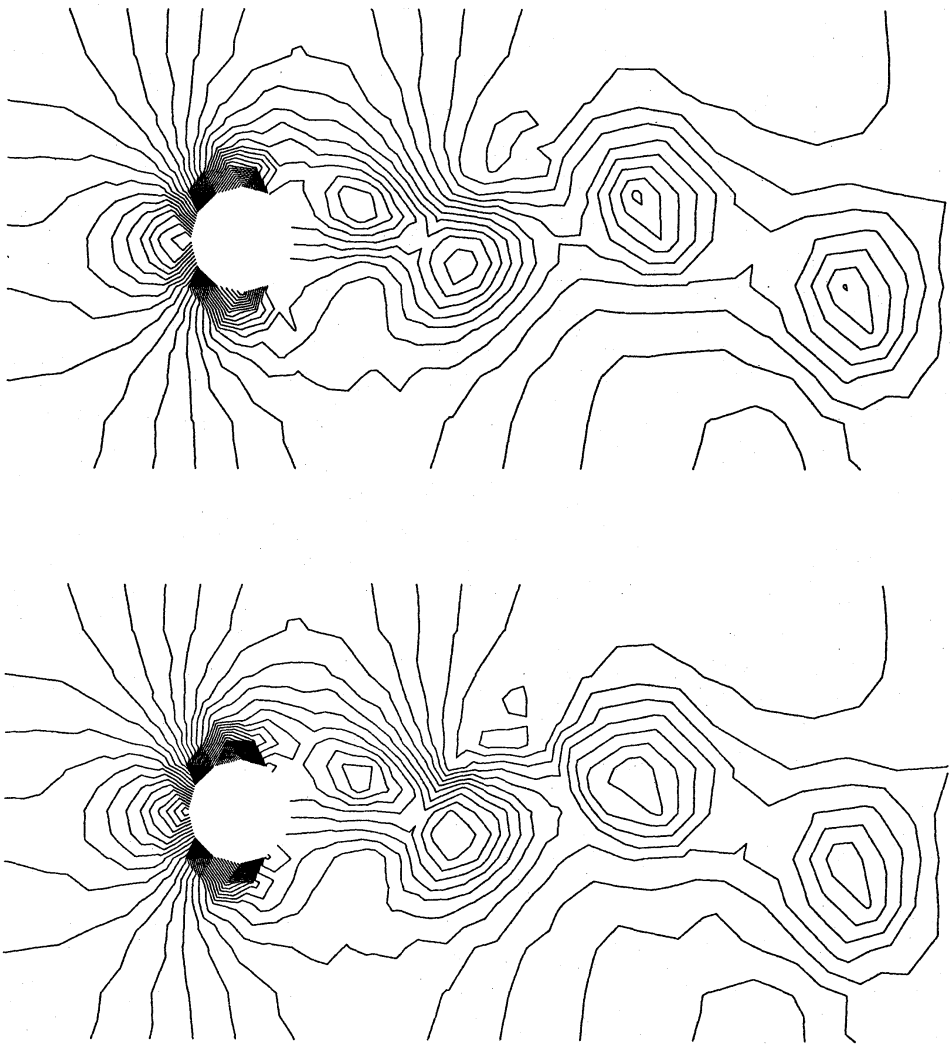

Figure 4: Pressure contours, $Re = 1000$, $t = 82.28$, $x_3 = 0$(upper) and 0.5(lower).

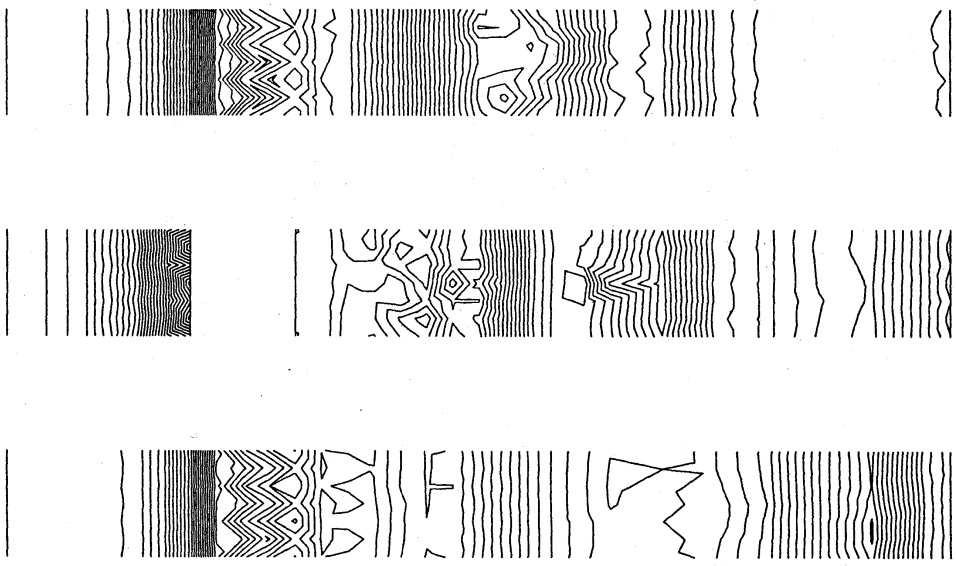

Figure 5: Pressure contours, $Re = 1000$, $t = 82.28$, x_2 =0.866, 0 and –0.866(from top).

Table 1: Measure of three-dimensional behavior.

Re	m	e_1	e_2	e_3	e_p
100	4	4.04e–2	6.44e–2	2.32e–2	5.11e–2
	6	3.57e–2	6.33e–2	1.86e–2	4.05e–2
1000	4	4.09e–2	6.95e–2	2.23e–2	5.22e–2
	6	3.66e–1	3.35e–1	1.49e–1	8.46e–2

$Re = 100$, these values decrease as m increases, therefore, the finite element solutions are considered to converge to a solution with a two-dimensional structure. On the other hand, we can see that the three-dimensional structure becomes clearer as m increases in the case of $Re = 1000$.

The subdivision of ω is not sufficient in the boundary layer for checking C_D quantitatively. We will do it using suitable finer subdivisions in the forthcoming paper.

5 Concluding Remarks

We have considered three-dimensional flows around a circular cylinder subject to the periodic conditions in the axial direction of the cylinder. We have computed them by the finite element scheme of third order accuracy and investigated the difference between two- and three-dimensional problems in the case of $Re = 100$ and $Re = 1000$.

In this paper we have set a priori the period $H = 1$. The consideration whether this choice is sufficient or not to approximate the original flow problem will be done in near future.

References

[1] M. Tabata, S. Fujima, An upwind finite element scheme for high-reynolds-number flows, *International Journal for Numerical Methods in Fluids*, 12, 305-322(1991).

[2] M. Tabata, S. Fujima, Finite-element analysis of high Reynolds number flows past a circular cylinder, *Journal of Computational and Applied Mathematics*, 38, 411-424(1991).

[3] T. Tamura, K. Kuwahara, Direct finite difference computation of turbulent flow around a circular cylinder, *Proc. Int. Symp. of Computational Fluid Dynamics*, Nagoya, 1989, 701-706.